Dalton Transactions

Synthesis and Characterization of M(II) (M = Mn, Fe, and Co) Azafulvene-amine Complexes and their Psuedohalide Derivatives

Journal:	*Dalton Transactions*
Manuscript ID:	DT-ART-03-2015-000985.R1
Article Type:	Paper
Date Submitted by the Author:	10-Apr-2015
Complete List of Authors:	Matson, Ellen; University of Illinois at Urbana-Champaign, School of Chemical Sciences Park, Yun Ji; University of Illinois at Urbana-Champaign, School of Chemical Sciences Bertke, Jeffery; University of Illinois at Urbana-Champaign, School of Chemical Sciences Fout, Alison; University of Illinois at Urbana-Champaign, School of Chemical Sciences

SCHOLARONE™
Manuscripts

Dalton Transactions RSCPublishing

ARTICLE

Synthesis and Characterization of M(II) (M = Mn, Fe and Co) Azafulvene Complexes and their X_3^- Derivatives.

Cite this: DOI: 10.1039/x0xx00000x

Received 00th January 2012,
Accepted 00th January 2012

DOI: 10.1039/x0xx00000x

www.rsc.org/

Ellen M. Matson [δ], Yun Ji Park [δ], Jeffery A. Bertke, and Alison R. Fout*[a]

The syntheses of M(II) (M = Mn, Fe, Co) complexes bearing the tris(5-cycloaminoazafulvene-2-methyl)amine ($H_3N(afa^{Cy})_3$) ligand in its datively coordinated, tautomeric form is reported. The metal-azafulvene complexes $[N(afa^{Cy})_3M](OTf)_2$ are generated in high yields, featuring a secondary coordination sphere composed of amino moieties from the ligand platform. To investigate the ability of the hydrogen bonding network to support hydrogen-bond accepting, coordinating anions, pseudohalide derivatives, $[N(afa^{Cy})_3MX](OTf)$ (X = NCS^-, NCO^-, N_3^-) were synthesized by exposure of $[N(afa^{Cy})_3M](OTf)_2$ to an equivalent of the corresponding salt, $[(^nBu)_4N](X)$. Structural characterization of the products reveals two isomorphs of the desired species. One complex features a single hydrogen bonding interaction with the pseudohalide, while the second compound has two H-bonds from the secondary coordination sphere to the coordinated anion. These complexes showcase the structural and electron flexibility of the ligand platform, presenting a scaffold capable of accessing a different number of hydrogen bonds for stabilizing a given moiety.

Introduction

Hydrogen-bonding plays an important role in the activation of small molecules by metalloproteins.[1-4] These intermolecular interactions have been shown to regulate biological activity by controlling the selectivity of substrates and/or by the stabilization of reactive intermediates.[5-7] This is exemplified in the active site of metalloproteins, where H-bonding networks and redox active amino acids affect both the physical and chemical properties correlated to the mode of action of the enzyme.[8-10] The relationship between primary and secondary coordination spheres for transition metal complexes has flourished in recent years as a result of X-ray crystallographic determination of structural nuances found in metalloproteins.[11-15] For example, H-bonding through histidine is essential for the binding of dioxygen in both hemoglobin and myoglobin.[16-18] Dioxygen is cleaved with the assistance of two hydrogen-bonding networks in Cytochrome P450, resulting in a high-valent iron centre.[3,19] In the Oxygen Evolving Complex of Photosystem II, a pendant tyrosine is involved in water oxidation.[13,20,21] These findings and others have stimulated the development of synthetic systems that feature H-bond donors/acceptors and/or redox active functional groups in the secondary coordination sphere.

Inspired by Nature, ligand systems featuring secondary coordination spheres have been developed to model the active site of metalloenzymes. Seminal contributions to the field of biomimetic inorganic chemistry have presented ligand architectures designed to coordinate to a metal centre, forming a H-bonding pocket for substrate activation and stabilization.[22-24] Early examples of complexes featuring H-bonding networks for the stabilization of biologically relevant, reactive intermediates are dominated by porphyrin-based ligand systems.[22,23,25] While these systems are excellent models of both primary and secondary coordination spheres of the heme active site, ligand syntheses can be multi-step and low-yielding.

As a result, a slew of non-heme metal complexes featuring non-covalent interactions in the secondary coordination sphere have been reported.[26-29] In particular, C_3-symmetric ligands have emerged as a popular platform due to their utility in stabilizing short-lived intermediates previously thought of as inaccessible. The lowering of the metal's symmetry from octahedral or tetrahedral to trigonal bipyramidal enhances the availability of additional non-bonding orbitals to stabilize highly reactive terminal ligands.[30] Capitalizing on the stabilizing effect of the primary coordination sphere, the Borovik group has synthesized a number of complexes featuring a urea-derived secondary coordination sphere.[7] Subsequent exposure of these complexes to molecular oxygen has resulted in the isolation of high-valent metal-oxo and hydroxyl species identified as intermediates along biological O_2 reduction pathways.[31-35] These reports have established that appropriately placed H-bonds are capable of regulating the microenvironment at the metal centre, mirroring the stabilizing influences H-bonding networks have within metalloenzymes.[1]

Understanding the interactions of the secondary coordination sphere with a variety of substrates is key to addressing various biologically relevant reaction mechanisms. Many enzymes readily react with O_2; however, to gain insight into this reaction, azide (N_3^-) can be used as a superoxide (O_2^-) surrogate.[36,37] Azides bind

similarly to the active site of the metalloenzyme as superoxide, but subsequent reactivity is limited. Substrates like azides, thiocyanates, and isocyanates contain multiple sites for H-bonding and allow for a detailed understanding of the non-covalent interactions between substrate and ligand platform. Furthermore, interactions of this type with a ligand featuring a hydrogen bonding cavity have not extensively been explored.[38]

Our group has recently developed tripodal ($H_3N(pi^{Cy})_3$)[39-41] and dipodal ($H_2^{Me}N(pi^{Cy})_2$)[42] ligand scaffolds that can undergo redox tautomerism to be either hydrogen bond donating in the azafulvene-amine tautomer (afa^{Cy}) or H-bond accepting when in the pyrrole-imine (pi^{Cy}) tautomeric form. In the tripodal ligand environment, the various pyrrole-imine arms of the ligand anionically coordinate to the metal centre, resulting in a hydrogen bond accepting pocket. Ligand tautomerization leads to dative coordination, featuring an azafulvene-amine hydrogen bond donating secondary coordination sphere, with amino moieties pointing away from the metal centre. Furthermore, our investigations have demonstrated that each arm of the ligand platform is capable of independent tautomerization.[40]

Intrigued by the positioning of the pendant N-Hs, our focus shifted to the generation of coordination complexes capable of engaging in hydrogen bonding interactions with the secondary coordination sphere of the ligand platform. To gain further insight into these effects we have traversed the periodic table of late first-row transition metals featuring various axial ligands to understand the role of our ligand platform and H-bonding on coordination chemistry. Herein we describe the synthesis and characterization of a family of azafulvene complexes, $[N(afa^{Cy})_3M(OTf)](OTf)$ [M = Mn (**1**), Fe (**2**), Co (**3**)]. Their subsequent reactivity with tetrabutyl ammonium salts, $[^nBu_4N]X$ (X = N_3, OCN and SCN) has also been explored to understand how the binding of anionic, axial substrates influence the coordination of the ligand and non-covalent interactions of the secondary coordination sphere. The surprising ability of the ligand to span multiple hydrogen bonding motifs presented herein demonstrates a novel, biomimetic scaffold capable of conformational changes to optimally stabilize M–X interactions.

Results and Discussion

Recently, we reported a family of iron and manganese complexes of the tripodal ligand, $H_3N(pi^{Cy})_3$.[40,41] As investigations into initial reactivity pointed towards the datively coordinated, azafulvene-amine derivatives as most reactive towards small molecule activation, the general application of the synthesis of $[N(afa^{Cy})_3]M(OTf)_2$ [M = Mn (**1**); Fe (**2**)] was applied to cobalt. Addition of the free ligand, $H_3N(pi^{Cy})_3$, to a THF solution of $Co(OTf)_2(MeCN)_2$ resulted in tautomerization of the ligand and formation of the desired complex, $[N(afa^{Cy})_3Co](OTf)_2$ (**3**), in quantitative yields. Analysis of complex **3** by ^{1}H NMR spectroscopy revealed paramagnetic resonances ranging from 58.72 to -2.54 ppm, and a broad feature at 88.10 ppm. Complex **3** has a similar, complicated splitting pattern to that reported previously for **2** (Figure S1).[40] Characterization of complex **3** by infrared spectroscopy revealed the expected bands at 3224 and 3291 cm^{-1}, corresponding to the N-H's of the tautomerized ligand platform. Additionally, an intense feature at 1637 cm^{-1} can be assigned to the C=N stretch of the azafulvene ring. These metrics compare favourably with that of complexes **1** (N-H: 3230, 3290 cm^{-1}; C=N: 1641 cm^{-1}) and **2** (N-H: 3224, 3291 cm^{-1}; C=N: 1636 cm^{-1}), suggesting analogous coordination environments for the variety of transition metals.[40,43]

Structural characterization of complex **3** by X-ray crystallography was accomplished by diffraction of crystals grown from a concentrated solution of THF layered with diethyl ether (1:1). Complex **3** is isomorphous to that of complexes **1** and **2**, with the metal centre positioned in the pocket of the ligand in a distorted trigonal bipyramidal geometry (Figure S2, Table S1). In the case of complex **3**, the cobalt centre is located similarly within the binding pocket as that of complexes **1** and **2**, best described by the Co1–N1 bond distance of 2.236(3) Å and N1–Co1–NX (X = 2, 3, 4) bond angles (ranging from 78.16(10) - 80.11(12)°); values which are within error of those reported for complexes **1** and **2**.[40,43] These values deviate from traditional coordination of trispyrryl-2-methylamine frameworks, where M1–N1 distances are shorter (2.144(1) – 2.172(2) Å) resulting in less acute N1–M1–NX bond angles (82.00(9)° – 83.84(6)°).[44] Solution magnetic properties of complexes **1-3** were determined by Evans' method and revealed, in all cases, a high-spin transition metal centre with μ_{eff} values of 5.88(7) μ_B (Mn), 5.35(2) μ_B (Fe) and 4.50(3) μ_B (Co), consistent with previously reported, high spin, trigonal bipyramidal M(II) complexes (M = Mn[45,46]; Fe[38,44,47] ; Co[48]).

With the family of $[N(afa^{Cy})_3M](OTf)_2$ complexes in hand, installation of a variety of anions possessing lone pairs of electrons capable of engaging in hydrogen bonding with the secondary coordination sphere was attempted. The purpose of the synthesis of these variants was to develop an increased understanding of the interaction of substrates with the secondary coordination sphere, to elucidate how the substrate can influence the coordination mode of the ligand scaffold. The pseudohalides thiocyanate, isocyanate and azide were selected due to their commercial availability and propensity to serve as model substrates for biological intermediates.[36,37] Binding of the linear functionality anionically to the metal centre has been shown to serve as a mimic for hydroxyl or peroxide intermediates, with lone pairs of electrons available for hydrogen bonding with the amino moieties of the ligand. Furthermore, these anions possess characteristic infrared stretching frequencies that provide electronic information on the interaction between metal centre and substrate.

In an effort to synthesize the desired $[N(afa^{Cy})_3MX]^+$ species (M = Mn, Fe, Co; X = NCS^-, NCO^-, N_3^-), salt metathesis with the corresponding $[^nBu_4N]X$ salt was employed for functionalization of complexes **1-3**. Initial experiments focused on the synthesis and characterization of the thiocyanate derivatives in order to understand the ligand's ability to H-bond with various anionic substrates without the complexity of variable coordination modes due to the

Scheme 1. Synthesis of $[N(afa^{Cy})_3M(X)]^+$ (X = NCS^-, NCO^-, N_3^-).

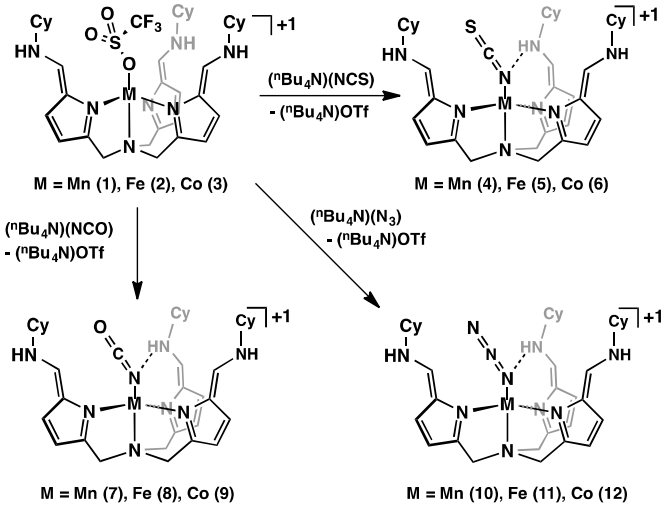

This journal is © The Royal Society of Chemistry 2012

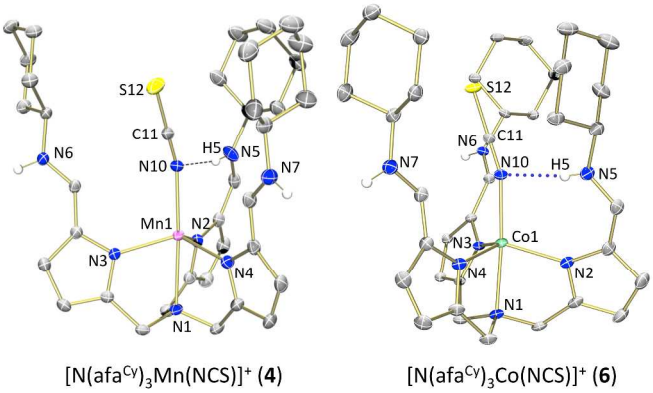

Figure 1. Molecular structures of **4** and **6** shown with 50% probability ellipsoids. Select hydrogen atoms, counter ions and solvent molecules have been removed for clarity.

ambidentate nature of the anion. Addition of an equivalent of [^{n}Bu$_4$N](NCS) to a THF slurry of the appropriate metal azafulvene precursor (complexes **1-3**) resulted in an instantaneous colour change. To ensure reaction completion, the mixtures were stirred for one hour, over which time the formation of a precipitate was observed, suspended as a fine powder in solution. Following work-up, the products, [N(afa^{Cy})$_3$M(NCS)](OTf) [M = Mn (**4**); Fe (**5**); Co (**6**)] were isolated as powders in quantitative yields. For the isolation of analytically pure samples, recrystallization was accomplished by slow diffusion of diethyl ether into a concentrated solution of DMA and acetonitrile (1:10). Magnetic moments of these new species are consistent with high-spin M(II) complexes [μ_{eff} = 5.96(12) μ_B (**4**), 5.32(3) μ_B (**5**), 4.31(2) μ_B (**6**)], however all values are slightly lower than that of the starting triflate complexes, suggesting a slight deviation in electronic environment upon coordination of (NCS$^-$). Complexes **4-6** were characterized by infrared spectroscopy to confirm installation of the new thiocyanate functional group. In all cases, the shifted, asymmetric stretch of the NCS$^-$ was noted by comparison to the values reported for the starting material [^{n}Bu$_4$N](NCS) (2060 cm^{-1}) ranging from 2016 to 2036 cm^{-1} (Table 1).

To gain insight into the structural parameters of the thiocycanate complexes, crystallographic characterization was performed on **4** and **6** (Figure 1, Table 1). In the case of the manganese and cobalt derivatives, crystals suitable for X-ray analysis were grown from concentrated solutions of DMA and acetonitrile in a 1:10 ratio, layered with diethyl ether. As the complexes are isomorphous, structural parameters for only the cobalt derivative (**6**) will be discussed. Upon refinement of the data, a pseudo trigonal bipyramidal geometry was noted for complex **6**. Co-NX (X = 1-4) distances are consistent with that of [N(afa^{Cy})$_3$Co]$^{2+}$ (**3**) starting material presented earlier, indicating analogous primary coordination interactions of the ancillary ligand platform with cobalt. Intraligand bond distances are of the appropriate values to confirm presence of the tautomeric amino-azafulvene form of the ligand backbone.

A new feature of the system was observed following installation of the thiocyanate anion, resulting from the rotation of a single arm of the ligand platform inward, giving rise to a H-bonding interaction between an amino moiety of the secondary coordination sphere and the nitrogen atom of the pseudohalide. The position of the hydrogen atom engaging in H-bonding with the axial ligand could be reliably determined and independently refined as a result of the high quality of the crystal. The N10-H5 distance of 2.23(3) Å and the N5–N10 distance of 2.926(2) Å are well within the range of distances established as hydrogen-bonding interactions (2.8 – 3.5 Å).[49] Further supporting the presence of a hydrogen bonding interaction is the nearly linear N5–H5–N10 bond angle of 169(3)°.

The observation of the formation of a new H-bonding interaction between the amino moiety and the substrate supports the hypothesis of the flexible nature of the ligand platform. Multiple isomorphs of the complexes can be invoked with a variety of secondary coordination sphere contributions, driven by the stabilization needs of the metal-substrate interaction. The participation of the ligand framework in H-bonding with the newly installed thiocyanate moiety is remarkable, as free rotation around the C=C bond of the azafulvene-amine tautomer is prohibited.

Table 1. Selected structural parameters of complexes **4,6-8, 11** and **12**.

Bond	**4** (Å) M = Mn # = 2	**6** (Å) M = Co # = 1	**7** (Å) M = Mn # = 1	**8** (Å) M = Fe # = 1	**11** (Å) M = Fe # = 1	**12** (Å) M = Co # = 2
M1-N1	2.3337(16)	2.2149(15)	2.3398(17)	2.2670(19)	2.256(2)	2.2283(17)
M1-N(pyr)	2.1427(18) – 2.1491(16)	2.0522(16) – 2.0587(16)	2.1201(17) – 2.1480(18)	2.079(7) – 2.110(4)	2.072(5) – 2.116(2)	2.0473(17) – 2.0652(17)
M1-NX0	2.1322(17)	2.0368(15)	2.1450(16)	2.076(5)	2.138(5)	2.0728(18)
N#0-H5	2.126(2)	2.23(3)	2.06[a]	2.13[a]	2.09(3)	2.03(3)
N#0···N5	2.993(2)	2.926(2)	2.93(2)	2.98(3)	2.898(9)	2.834(3)
N#0-H5-N5	168(1)°	169(3)°	175.7[a]	161.4[a]	170(3)°	176(3)°
N-H stretch	3218, 3280 cm^{-1}	3207, 3286 cm^{-1}	3202, 3288 cm^{-1}	3221, 3289 cm^{-1}	3203, 3286 cm^{-1}	3206, 3291 cm^{-1}
C=N stretch	1646 cm^{-1}	1644 cm^{-1}	1640 cm^{-1}	1640 cm^{-1}	1646 cm^{-1}	1643 cm^{-1}
IR stretch, X	2016 cm^{-1}	2036 cm^{-1}	2178 cm^{-1}	2180 cm^{-1}	2057 cm^{-1}	2060 cm^{-1}
μ_{eff}	5.96(12) μ_B	4.31(2) μ_B	5.90(11) μ_B	5.14(3) μ_B	5.14(3) μ_B	4.39(4) μ_B

[a]NX0···H5 bond distance and NX0···H5-N5 bond angles are calculated metrics included for comparison purposes.

Figure 2. Molecular structures of complexes **7**, **8**, **11** and **12** shown with 50% probability ellipsoids. Select hydrogen atoms, counter ions and solvent molecules have been removed for clarity.

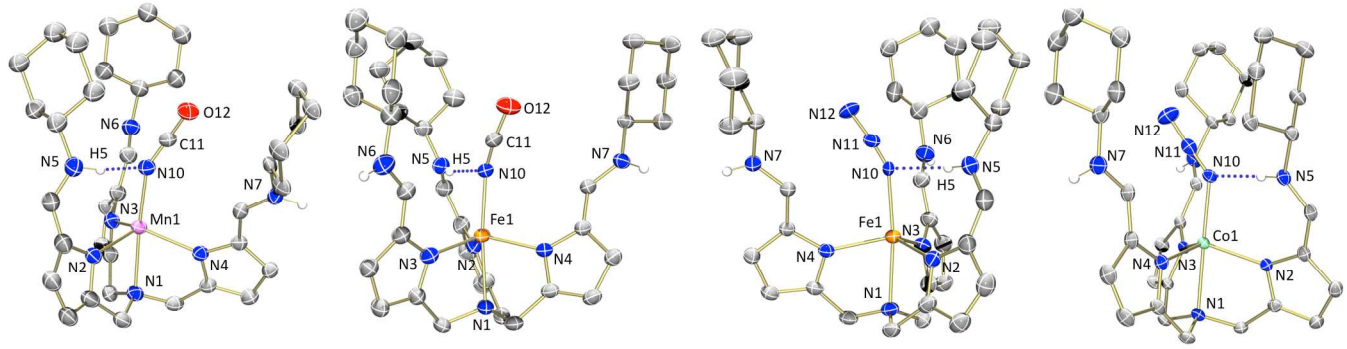

$[N(afa^{Cy})_3Mn(NCO)]^+$ (**7**) $[N(afa^{Cy})_3Fe(NCO)]^+$ (**8**) $[N(afa^{Cy})_3Fe(N_3)]^+$ (**11**) $[N(afa^{Cy})_3Co(N_3)]^+$ (**12**)

Interested in investigating the electronic and structural properties of isocyanate derivatives of the metal azafulvene complexes, synthesis was accomplished by addition of an equivalent of $[^nBu_4N][NCO]$ to $[N(afa^{Cy})_3M]^{2+}$ [M = Mn (**1**), Fe (**2**), Co (**3**)]. Primary motivation for the exploration of the oxygen-containing pseudohalide was to generate a complex resembling the structural properties of a peroxide moiety, with a M–O single bond stabilized through H-bonding interactions. Following salt metathesis, installation of the psuedohalide was confirmed by infrared spectroscopy; $[N(afa^{Cy})_3M(NCO)]^+$ bears sharp bands assigned to a bound isocyanate moiety (M = Mn, 2178 cm^{-1}; Fe, 2180 cm^{-1}; Co, 2186 cm^{-1}), shifted from that of the starting material, $[^nBu_4N](NCO)$ (2160 cm^{-1}).

Crystallographic characterization of the manganese and iron complexes of the isocyanate species, $[N(afa^{Cy})_3M(NCO)](OTf)$ [M = Mn (**7**) and Fe (**8**)] was possible by diffraction of single crystals grown from a concentrated solution of acetonitrile and DMA (10:1) layered with diethyl ether (Figure 2). In the case of both complexes **7** and **8**, a single molecule was identified in the asymmetric unit, consisting of two disordered species. In the major component (Mn = 68%; Fe = 64%), a single arm of the tripodal framework has been rotated inwards, engaging in hydrogen bonding with the nitrogen located closest to the metal centre in the axial isocyanate substituent. The minor component has two arms of the ligand platform engaging in hydrogen bonding with the substrate. Complexes **7** and **8** are isostructural with one another, crystallizing in identical unit cells. For simplification of the subsequent discussion, structural parameters of complex **8** will be discussed (summary of pertinent bond distances and angles for complexes **7** and **8** are summarized in Table 1).

Structural refinement of complex **8** revealed a distorted trigonal bipyramidal geometry about the metal centre, similar to that of the thiocyanate complexes, **4** and **6.** The isocyanate moiety has replaced the triflate as anticipated, driving a single N–H bond to rotate inward stabilizing the substrate via a new hydrogen bonding interaction. The disorder of a single arm of the ligand framework in the crystal structure gives rise to a metal-isocyanate complex where two ligand arms are now participating in H-bonding (Figure 3). To accommodate this increase in ligand-anion H-bonding, the isocyanate moiety is positioned at a slightly more acute angle (Fe1–N10B–C11B = 142(2)°) in comparison to the major component of the crystal structure (Fe1–N10–C11 = 148.2(15)°). The entire arm of the ligand engaging in the additional H-bond with the isocyanate anion is distorted, indicating a significant structural change to accommodate the second N10⋯H5–N5 interaction. The ability of the ligand to participate in this remarkable structural transformation highlights the ability of this tripodal platform to adequately mimic amino acid binding sites present in metalloenzymes by adjusting the number of H-bonding interactions to best suit the stabilization needs of the complex.

Figure 3. Disorder in structure of $[N(afa^{Cy})_3Fe(NCO)]^+$ (**8**).

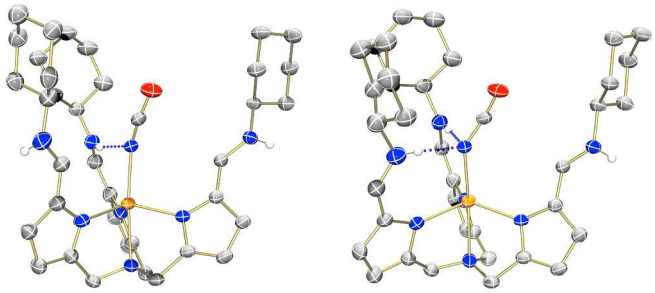

Intrigued by the participation of the secondary coordination sphere in stabilization of the thiocyanate and isocyanate moieties, synthesis of the structurally analogous metal-azide complexes was subsequently explored. Azide moieties have been shown to spectroscopically mimic metal peroxide species and have been utilized to investigate the electronic properties of proposed intermediates in enzymatic pathways. In recent EPR spectroscopic studies, Rivera and coworkers observed the presence of an iron(III)peroxo species,[36,37] while the electronically similar species were studied utilizing azide and cyanide ligands as models for the reactive peroxo substrate. Additionally, metal azide complexes are well-established precursors for metal nitrides. As our research group is primarily interested in the utilization of secondary coordination spheres for the stabilization of intermediates along biologically relevant mechanistic pathways including water oxidation, oxygen reduction, or nitrogen reduction, the synthesis of a series of metal azide complexes was explored.

The synthesis and purification of the azide derivatives were accomplished in a similar fashion to that discussed for the synthesis of complexes **4-9**. Following work-up, the products, $[N(afa^{Cy})_3M(N_3)](OTf)$ [M = Mn (**10**); Fe (**11**); Co (**12**)] were isolated as powders in quantitative yields. Magnetic properties of the products revealed similar electronic states to that of the respective starting materials. For complexes **10-12**, room temperature solution magnetic moments of 5.88(4) μ_B (**10**), 5.14(3) μ_B (**11**) and 4.39(14) μ_B (**12**), are again consistent with high-spin, M(II) species. The effective magnetic moments of complexes **10-12** also resemble those

This journal is © The Royal Society of Chemistry 2012

obtained for the corresponding thiocyanate or isocyanate derivatives, complexes **4-9**.

To confirm the installation of the azide moiety, infrared spectroscopy was employed to determine the stretching frequency of the coordinated [N_3^-]. For complexes **10-12**, strong bands were located at 2067, 2057, and 2060 cm^{-1}, respectively. These values are shifted from that of the azide starting material, [$^nBu_4N$]N_3 (2022 cm^{-1}). The C=N stretches observed in the infrared spectra of complexes **10-12** (1640 – 1655 cm^{-1}) are similar to that of the tripodal starting materials (1636 – 1639 cm^{-1}), and are consistent with the dative azafulvene-amine binding mode of the tripodal ligand.[39,40] For complexes **10-12**, two broad bands corresponding to the N–H stretches of the secondary amino groups were located between 3203-3294 cm^{-1} per compound, suggesting multiple H-bonding domains within the products.

Crystallographic characterization was performed on multiple azide complexes, [N(afa^{Cy})$_3$M(N_3)](OTf) where M = Fe (**11**) and Co (**12**). In the case of iron, a single molecule was identified in the independent unit, consisting of two disordered species. Similar to the isocyanate derivatives, in the major component of **11** (64%), a single arm of the tripodal framework has been rotated inwards, engaging in H-bonding with the lone pair of electrons of the nitrogen located closest to the metal centre in the axial azide substituent. The minor component has two arms of the ligand platform engaging in H-bonding with the substrate. Structural parameters were obtained for the cobalt derivative (**12**), however, multiple molecules within the independent unit cell prevented a clear understanding of disorder of the azide moiety and ligand platform. For comparison, pertinent bond lengths and angles of **11** and **12** are summarized in Table 1.

A structural model was resolved in the case of [N(afa^{Cy})$_3$Fe(N_3)]$^+$ in which the tripodal ligand platform and azide ligand form a trigonal bipyramidal coordination geometry about the metal centre (Figure 2, Table 1). The coordination geometry about iron is analogous to that of complex **8**. The Fe1–N10 bond distance of 2.084(4) Å is well within reported five-coordinated anionic iron-nitrogen (Fe–N_3) interactions (1.953(5)–2.134(5) Å),[50-53] and compares favourably with the isocyanate species, **8**, reported herein (2.137(5) Å). As in the case of the metal isocyanate species, complex **11** possesses multiple coordination modes of the axial ligand, influencing the number of H-bonding interactions between the amino moieties and the nitrogen atom of the azide bound to the iron centre.

The synthesis of metal azide complexes by salt metathesis is a common strategy to access precursors to metal nitride species. In recent work, Smith and coworkers have presented the synthesis and characterization of the terminal Fe(IV) nitride species, generated by photolysis of a Fe(II) azide complex, PhB(^{t}Bulm)$_3$FeN_3.[54,55] Likewise, Meyer and coworkers have recently reported a Co(II) azide complex that releases an equivalent of N_2 to form a transient Co(IV) nitride upon exposure to UV light.[56] Despite extensive attempts to access the desired complexes "[N(afa^{Cy})$_3$MN]" via thermolysis, photolysis and chemical reduction, isolation of the terminal nitride remains elusive.

Experimental

General Considerations. All manipulations were carried out in the absence of water and dioxygen using standard Schlenk techniques, or in an MBraun inert atmosphere drybox under a dinitrogen atmosphere except where specified otherwise. All glassware was oven dried for a minimum of 8 h and cooled in an evacuated antechamber prior to use in the drybox. Solvents were dried and deoxygenated on a Glass Contour System (SG Water USA, Nashua, NH) and stored over 4 Å molecular sieves purchased from Strem following literature procedure prior to use. H_3N(pi^{Cy})$_3$,[40] [N(afa^{Cy})M(OTf)](OTf) [M = Mn[43] (**1**), Fe (**2**)[40]], and Co(OTf)$_2$(MeCN)$_2$[57] were prepared according to literature procedures. [$^nBu_4N$](X) (X = NCS, NCO, N_3) were purchased from Sigma Aldrich and used as received.

^{1}H and ^{19}F NMR Spectra were recorded at room temperature on a Varian spectrometer operating at 500 MHz (^{1}H NMR) and 470 MHz (^{19}F NMR) and referenced to the residual solvent resonance (δ in parts per million, and *J* in Hz). Infrared spectra were recorded using a Perkin-Elmer Frontier FT-IR spectrophotometer equipped with a KRS5 Thallium Bromide/Iodide Universal Attenuated Total Reflectance accessory. Elemental analysis was performed by Complete Analysis Laboratories, Inc. in Parsippany, NJ and the University of Illinois at Urbana-Champaign School of Chemical Sciences Microanalysis Laboratory in Urbana, IL. All structures were collected on a Bruker APEX II Duo three-circle goniometer equipped with an Oxford cryostream cooling device.

Preparation of [N(afa^{Cy})$_3$Co](OTf)$_2$ (3). A 20 mL scintillation vial was charged with Co(OTf)$_2$(MeCN)$_2$ (0.044 g, 0.100 mmol) and approximately 10 mL of tetrahydrofuran. With vigorous stirring, H_3N(pi^{Cy})$_3$ (0.060 g, 0.103 mmol) was added as a solid by difference. Addition of H_3N(pi^{Cy})$_3$ results in the dissolution of the pale pink solid of the starting material, giving rise to a translucent, pink-red solution. Following removal of volatiles, the pink oil was washed with diethyl ether. The mixture was stirred for one hour, after which time solvents were removed under reduced pressure. The product, **3**, was isolated as a pink powder in quantitative yields (0.098 g, 0.098 mmol, 97%). Crystals of **3** suitable for X-ray analysis were grown at room temperature from a concentrated solution of acetonitrile and tetrahydrofuran (1:2) layered with diethyl ether. Analysis for $CoC_{38}H_{51}N_7S_2F_6O_6$•$OC_4H_8$: Calcd. C, 48.62; H, 6.03; N, 9.93. Found C, 48.72; H, 5.43; N, 10.38. μ_{eff} = 4.50(3) μ_B. IR: 1637 cm^{-1} (C=N), 3224, 3291 cm^{-1} (NH).

General procedure for synthesis of [N(afa^{Cy})$_3$M(NCS)](OTf). A 20 mL scintillation vial was charged with [N(afa^{Cy})$_3$M](OTf)$_2$ [M = Mn (0.093 g, 0.100 mmol); Fe 0.093 g, 0.100 mmol); Co (0.094 g, 0.100 mmol)] and approximately 10 mL of tetrahydrofuran. With vigorous stirring, [$^nBu_4N$][NCS] (0.030 g, 0.102 mmol) was weighed and added as a white solid. The mixture was stirred for one hour, after which time solvents were removed under reduced pressure.

[N(afa^{Cy})$_3$Mn(NCS)](OTf) (4). The resulting yellow powder was washed three times with diethylether to remove the byproduct, tetrabutylammonium triflate. The product, **4**, was isolated as a yellow powder in quantitative yields (0.079 g, 0.094 mmol, 94%). Yellow crystals suitable for X-ray analysis were grown from acetonitrile-DMA mixture(10:1) layered with diethyl ether. Analysis for $MnC_{37}H_{51}N_8O$•SO_3CF_3: Calcd. C, 55.13; H, 6.21; N, 13.54. Analysis for $MnC_{37}H_{51}N_8S$•SO_3CF_3: Calcd. C, 54.08; H, 6.09; N, 13.28. Found C, 53.75; H, 6.21; N, 12.80. μ_{eff} = 5.96(12) μ_B. IR: 1646 cm^{-1} (C=N), 2016 cm^{-1} (NCS), 3218, 3280 cm^{-1} (NH).

[N(afa^{Cy})$_3$Fe(NCS)](OTf) (5). The resulting orange powder was washed three times with diethyl ether to remove tetrabutylammonium triflate. The product, **5**, was isolated as an orange solid in quantitative yields. Analytically pure product was isolated by recrystallization from a concentrated acetonitrile and DMA (10:1) mixture layered with diethylether. Analysis for $FeC_{37}H_{51}N_8S$•SO_3CF_3: Calcd. C, 54.02; H, 6.08; N, 13.26. Found C, 54.27; H, 6.44; N, 12.86. μ_{eff} = 5.32(3) μ_B. IR: 1644 cm^{-1} (C=N), 2036 cm^{-1} (NCS), 3207, 3286 cm^{-1} (NH).

[N(afa^{Cy})$_3$Co(NCS)](OTf) (6). The purple powder was washed three times with THF to remove the byproduct tetrabutylammonium triflate. The product, **6**, was isolated as a purple solid in quantitative

yields (0.082 g, 0.097 mmol, 97 %). Purple-pink crystals suitable for X-ray analysis were grown from a concentrated acetonitrile and DMA solution layered with diethylether. Analysis for $CoC_{37}H_{51}N_8O\bullet SO_3CF_3\bullet OC_4H_8$: Calcd. C, 54.83; H, 6.46; N, 12.18. Found C, 54.43; H, 6.57; N, 12.48. μ_{eff} = 4.31(2) μ_B. IR: 1642 cm^{-1} (C=N), 2016 cm^{-1} (NCS), 3217 cm^{-1} (NH).

General procedure for the synthesis of $[N(afa^{Cy})_3M(NCO)](OTf)$. A 20 mL scintillation vial was charged with $[N(afa^{NCy})_3M](OTf)_2$ [M = Mn (0.093g, 0.100mmol); Fe (0.093 g, 0.100 mmol); Co (0.094 g, 0.100 mmol)] and approximately 10 mL of tetrahydrofuran. With vigorous stirring, $[^nBu_4N][OCN]$ (0.029 g, 0.102 mmol) was weighed and added as a white solid. The mixture was stirred for one hour, after which time solvents were removed under reduced pressure.

$[N(afa^{Cy})_3Mn(NCO)](OTf)$ (7). The resulting yellow powder was washed three times with diethylether to remove the byproduct, tetrabutylammonium triflate. The product, **7**, was isolated as a yellow powder in quantitative yields (0.079 g, 0.096 mmol, 96%). Yellow crystals suitable for X-ray analysis were grown from acetonitrile-DMA mixture(10:1) layered with diethyl ether. Analysis for $MnC_{37}H_{51}N_8O\bullet SO_3CF_3$: Calcd. C, 55.13; H, 6.21; N, 13.54. Found C, 55.37; H, 6.34; N, 13.05.. μ_{eff} = 5.90(11) μ_B. IR: 1640 cm^{-1} (C=N), 2178 cm^{-1} (NCO), 3202 cm^{-1} (NH).

$[N(afa^{Cy})_3Fe(NCO)](OTf)$ (8). The resulting orange powder was washed with a 1:1 diethylether and THF mixture to remove the byproduct, tetrabutylammonium triflate. The remaining solid was dissolved in acetonitrile and DMA (10:1) and layered with diethyl ether, resulting in orange crystals of analytically pure product (0.053 g, 0.064 mmol, 64 %). Analysis for $FeC_{37}H_{51}N_8O\bullet SO_3CF_3$: Calcd. C, 55.07; H, 6.20; N, 13.52. Found C, 55.15; H, 6.28; N, 13.34. μ_{eff} = 5.14(3) μ_B. IR: 1640 cm^{-1} (C=N), 2180 cm^{-1} (NCO), 3221, 3289 cm^{-1} (NH).

$[N(afa^{Cy})_3Co(NCO)](OTf)$ (9). The resulting purple powder was washed three times with diethylether. To isolate analytically pure sample, the product was dissolved in acetonitrile and DMA (10:1) and layered with diethyl ether. Purple crystals of the desired product were grown over 24 hours (0.057 g, 0.068 mmol, 68 %). Analysis for $CoC_{37}H_{51}N_8O\bullet SO_3CF_3$: Calcd. C, 54.56; H, 6.18; N, 13.47. Found C, 54.08; H, 6.37; N, 12.89. μ_{eff} = 4.42(1) μ_B. IR: 1639 cm^{-1} (C=N), 2186 cm^{-1} (NCO), 3225, 3282 cm^{-1} (NH).

General procedure for synthesis of $[N(afa^{Cy})_3M(N_3)](OTf)$. A 20 mL scintillation vial was charged with $[(afa^{NCy})_3M](OTf)_2$ [M = Mn (0.093g, 0.100 mmol); Fe 0.093 g, 0.100 mmol); Co (0.094 g, 0.100 mmol)] and approximately 10 mL of tetrahydrofuran. With vigorous stirring, $[^nBu_4N][N_3]$ (0.029 g, 0.102 mmol) was weighed by difference and added as a white solid. The mixture was stirred for one hour, after which time solvents were removed under reduced pressure.

$[N(afa^{Cy})_3Mn(N_3)](OTf)$ (10). The resulting pale yellow powder was washed three times with a 1:1 diethylether and THF mixture to remove the byproduct, tetrabutylammonium triflate. The remaining powder was dried under reduced pressure to yield the product in high yields (0.077 g, 0.094 mmol, 94%). Analysis for $[MnC_{36}H_{51}N_{10}\bullet SO_3CF_3]\bullet C_4H_8O$: Calcd. C, 54.72; H, 6.61; N, 15.56. Found C, 54.40; H, 6.50; N, 15.59. μ_{eff} = 5.88(4) μ_B. IR: 1655 cm^{-1} (C=N), 2067 cm^{-1} (N_3), 3216 cm^{-1} (NH).

$[N(afa^{Cy})_3Fe(N_3)](OTf)$ (11). The resulting orange powder was washed three times with diethylether to remove the byproduct, tetrabutylammonium triflate. The product was recrystallized by layering a concentrated solution of acetonitrile and dimethylformamide (10:1) with diethyl ether. Orange crystals suitable for X-ray analysis were grown from a THF-DMA mixture (10:2) layered with diethyl ether. Analysis for $[FeC_{36}H_{51}N_{10}\bullet SO_3CF_3]\bullet C_4H_8O$: Calcd. C, 55.26; H, 6.51; N, 15.34. Found C, 54.93; H, 6.65; N, 15.75. μ_{eff} = 5.14(3) μ_B. IR: 1646 cm^{-1} (C=N), 2057 cm^{-1} (N_3), 3203, 3286 cm^{-1} (NH).

$[N(afa^{Cy})_3Co(N_3)](OTf)$ (12). The resulting purple powder was washed three times with diethyl ether to remove the byproduct, tetrabutylammonium triflate. Analytically pure sample was obtained by crystallizing complex **12** from a concentrated acetonitrile-DMA mixture layered with diethylether. Crystals of complex **12** suitable for X-ray analysis were grown from a solution of THF-DMA layered with diethyl ether. Analysis for $[CoC_{36}H_{51}N_{10}\bullet SO_3CF_3]\bullet C_4H_8O$: Calcd. C, 53.42; H, 6.18; N, 16.84. Found C, 53.31; H, 6.11; N, 16.59. μ_{eff} = 4.39(4) μ_B. IR: 1643 cm^{-1} (C=N), 2060 cm^{-1} (N_3), 3206, 3291 cm^{-1} (NH).

Conclusions

A series of azafulvene complexes, $[N(afa^{NCy})_3M(OTf)](OTf)$ and their subsequent reactivity with tetrabutyl ammonium salts, $[N(Bu)_4]X$ (X = NCS, NCO and N_3) has been described in order to understand the effects various bound substrates have on the hydrogen bonding within the secondary coordination sphere. All of the complexes exhibit a single hydrogen bond from the ligand scaffold to the substrate. However, when either azide or isocyanate is bound a secondary component was characterized by X-ray crystallography, whereby two arms of the tripodal ligand hydrogen bonds to the apical nitrogen of the substrate. The addition of a second hydrogen bond is not simple; as free rotation around the C=C bond of the azafulvene-amine tautomer is prohibited. Tautomerization of the ligand scaffold allows for this fluxional behaviour of the ligand platform, resulting in variable hydrogen bonding motifs.

Acknowledgements

The authors gratefully acknowledge Dr. Danielle Gray for crystallographic help, an NSF CAREER award to ARF, and the University of Illinois at Urbana Champaign for financial support.

Notes and references

[a] School of Chemical Sciences, University of Illinois at Urbana-Champaign, 600 S. Mathews Ave. Urbana, Illinois 61801, United States.

[δ] denotes authors contributed equally.

Electronic Supplementary Information (ESI) available: including spectroscopic and crystallographic details. CCDC 1049539-1049545. See DOI: 10.1039/b000000x/

(1) Baik, M.-H.; Newcomb, M.; Friesner, R. A.; Lippard, S. J. *Chem. Rev.* **2003**, *103*, 2385.
(2) Costas, M.; Mehn, M. P.; Jensen, M. P.; Que, L. *Chem. Rev.* **2004**, *104*, 939.
(3) Groves, J. T. *J. Inorg. Biochem.* **2006**, *100*, 434.
(4) Kovacs, J. A. *Chem. Rev.* **2004**, *104*, 825.
(5) Fitzpatrick, P. F. *Biochemistry* **2003**, *42*, 14083.
(6) Himo, F.; Siegbahn, P. E. M. *Chem. Rev.* **2003**, *103*, 2421.
(7) Borovik, A. S. *Acc. Chem. Res.* **2005**, *38*, 54.
(8) Holm, R. H.; Kennepohl, P.; Solomon, E. I. *Chem. Rev.* **1996**, *96*, 2239.
(9) Ozaki, S.-i.; Roach, M. P.; Matsui, T.; Watanabe, Y. *Acc. Chem. Res.* **2001**, *34*, 818.
(10) Mukai, M.; Nagano, S.; Tanaka, M.; Ishimori, K.; Morishima, I.; Ogura, T.; Watanabe, Y.; Kitagawa, T. *J. Am. Chem. Soc.* **1997**, *119*, 1758.

This journal is © The Royal Society of Chemistry 2012

(11) Dawson, J. *Science* **1988**, *240*, 433.
(12) Zouni, A.; Witt, H.-T.; Kern, J.; Fromme, P.; Krauss, N.; Saenger, W.; Orth, P. *Nature* **2001**, *409*, 739.
(13) Yano, J.; Kern, J.; Sauer, K.; Latimer, M. J.; Pushkar, Y.; Biesiadka, J.; Loll, B.; Saenger, W.; Messinger, J.; Zouni, A.; Yachandra, V. K. *Science* **2006**, *314*, 821.
(14) Williams, P. A.; Fulop, V. *Nature* **1997**, *389*, 406.
(15) Fülöp, V.; Phizackerley, R. P.; Soltis, S. M.; Clifton, I. J.; Wakatsuki, S.; Erman, J.; Hajdu, J.; Edwards, S. L. *Structure* **1994**, *2*, 201.
(16) Springer, B. A.; Sligar, S. G.; Olson, J. S.; Phillips, G. N., Jr. *Chem. Rev.* **1994**, *94*, 699.
(17) Perutz, M. F.; Fermi, G.; Luisi, B.; Shaanan, B.; Liddington, R. C. *Acc. Chem. Res.* **1987**, *20*, 309.
(18) Sono, M.; Roach, M. P.; Coulter, E. D.; Dawson, J. H. *Chem. Rev.* **1996**, *96*, 2841.
(19) Gerber, N. C.; Sligar, S. G. *J. Am. Chem. Soc.* **1992**, *114*, 8742.
(20) Loll, B.; Kern, J.; Saenger, W.; Zouni, A.; Biesiadka, J. *Nature* **2005**, *438*, 1040.
(21) McEvoy, J. P.; Brudvig, G. W. *Chem. Rev.* **2006**, *106*, 4455.
(22) Collman, J. P.; Zhang, X.; Wong, K.; Brauman, J. I. *J. Am. Chem. Soc.* **1994**, *116*, 6245.
(23) Yeh, C.-Y.; Chang, C. J.; Nocera, D. G. *J. Am. Chem. Soc.* **2001**, *123*, 1513.
(24) Kitajima, N.; Komatsuzaki, H.; Hikichi, S.; Osawa, M.; Moro-oka, Y. *J. Am. Chem. Soc.* **1994**, *116*, 11596.
(25) Momenteau, M.; Reed, C. A. *Chem. Rev.* **1994**, *94*, 659.
(26) Soo, H. S.; Komor, A. C.; Iavarone, A. T.; Chang, C. J. *Inorg. Chem.* **2009**, *48*, 10024.
(27) Widger, L. R.; Davies, C. G.; Yang, T.; Siegler, M. A.; Troeppner, O.; Jameson, G. N. L.; Ivanović-Burmazović, I.; Goldberg, D. P. *J. Am. Chem. Soc.* **2014**, *136*, 2699.
(28) Kendall, A. J.; Zakharov, L. N.; Gilbertson, J. D. *Inorg. Chem.* **2010**, *49*, 8656.
(29) Zhao, M.; Wang, H.-B.; Ji, L.-N.; Mao, Z.-W. *Chem. Soc. Rev.* **2013**, *42*, 8360.
(30) Saouma, C. T.; Peters, J. C. *Coord. Chem. Rev.* **2011**, *255*, 920.
(31) Borovik, A. S. *Acc. Chem. Res.* **2004**, *38*, 54.
(32) MacBeth, C. E.; Golombek, A. P.; Young, V. G.; Yang, C.; Kuczera, K.; Hendrich, M. P.; Borovik, A. S. *Science* **2000**, *11*, 938.
(33) Shook, R. L.; Peterson, S. M.; Greaves, J.; Moore, C.; Rheingold, A. L.; Borovik, A. S. *J. Am. Chem. Soc.* **2011**, *133*, 5810.
(34) Shirin, Z.; Hammes, B. S.; Young, V. G.; Borovik, A. S. *J. Am. Chem. Soc.* **2000**, *122*, 1836.
(35) Shook, R. L.; Borovik, A. S. *Chem. Commun.* **2008**, 6095.
(36) Rivera, M.; Caignan, G. A.; Astashkin, A. V.; Raitsimring, A. M.; Shokhireva, T. K.; Walker, F. A. *J. Am. Chem. Soc.* **2002**, *124*, 6077.
(37) Caignan, G. A.; Deshmukh, R.; Zeng, Y.; Wilks, A.; Bunce, R. A.; Rivera, M. *J. Am. Chem. Soc.* **2003**, *125*, 11842.
(38) Reid, S. D.; Wilson, C.; Blake, A. J.; Love, J. B. *Dalton Transactions* **2010**, *39*, 418.
(39) Matson, E. M.; Park, Y. J.; Fout, A. R. *J. Am. Chem. Soc.* **2014**, *136*, 17398.
(40) Matson, E. M.; Bertke, J. A.; Fout, A. R. *Inorg. Chem.* **2014**, *53*, 4450.
(41) Park, Y. J.; Matson, E. M.; Nilges, M. J.; Fout, A. R. *Chem. Commun.* **2015**.
(42) Matson, E. M.; Gordon, Z.; Lin, B.; Nilges, M. J.; Fout, A. R. *Dalton Transactions* **2014**, *43*, 16992.
(43) Park, Y. J.; Matson, E. M.; Nilges, M. J.; Fout, A. R. *Chem. Commun.* **2015**, *51*, 5310.
(44) Harman, W. H.; Harris, T. D.; Freedman, D. E.; Fong, H.; Chang, A.; Rinehart, J. D.; Ozarowski, A.; Sougrati, M. T.; Grandjean, F.; Long, G. J.; Long, J. R.; Chang, C. J. *J. Am. Chem. Soc.* **2010**, *132*, 18115.
(45) Gupta, R.; MacBeth, C. E.; Young, V. G.; Borovik, A. S. *J. Am. Chem. Soc.* **2002**, *124*, 1136.
(46) Lu, C. C.; Peters, J. C. *Inorg. Chem.* **2006**, *45*, 8597.
(47) Harman, W. H.; Chang, C. J. *J. Am. Chem. Soc.* **2007**, *129*, 15128.
(48) Hossain, M. J.; Sakiyama, H. *Inorg. Chim. Acta* **2002**, *338*, 255.
(49) *Hydrogen Bonding in Organic Synthesis*; Wiley-VCH Verlag GmbH & Co. KGaA, 2009.
(50) Zhang, Y.; Hallows, W. A.; Ryan, W. J.; Jones, J. G.; Carpenter, G. B.; Sweigart, D. A. *Inorg. Chem.* **1994**, *33*, 3306.
(51) Chun, H.; Bill, E.; Weyhermüller, T.; Wieghardt, K. *Inorg. Chem.* **2003**, *42*, 5612.
(52) Davies, S. C.; Durrant, M. C.; Hughes, D. L.; Richards, R. L.; Sanders, J. R. *J. Chem. Soc., Dalton Trans.* **2000**, 4694.
(53) Liu, Z.-D.; Tan, M.-Y.; Zhu, H.-L. *Acta Crystallographica Section E* **2004**, *60*, m910.
(54) Scepaniak, J. J.; Young, J. A.; Bontchev, R. P.; Smith, J. M. *Angew. Chem. Int. Ed.* **2009**, *48*, 3158.
(55) Scepaniak, J. J.; Vogel, C. S.; Khusniyarov, M. M.; Heinemann, F. W.; Meyer, K.; Smith, J. M. *Science* **2011**, *331*, 1049.
(56) Zolnhofer, E. M.; Käß, M.; Khusniyarov, M. M.; Heinemann, F. W.; Maron, L.; van Gastel, M.; Bill, E.; Meyer, K. *J. Am. Chem. Soc.* **2014**.
(57) Seitz, M.; Kaiser, A.; Powell, D. R.; Borovik, A. S.; Reiser, O. *Adv. Synth. Catal.* **2004**, *346*, 737.

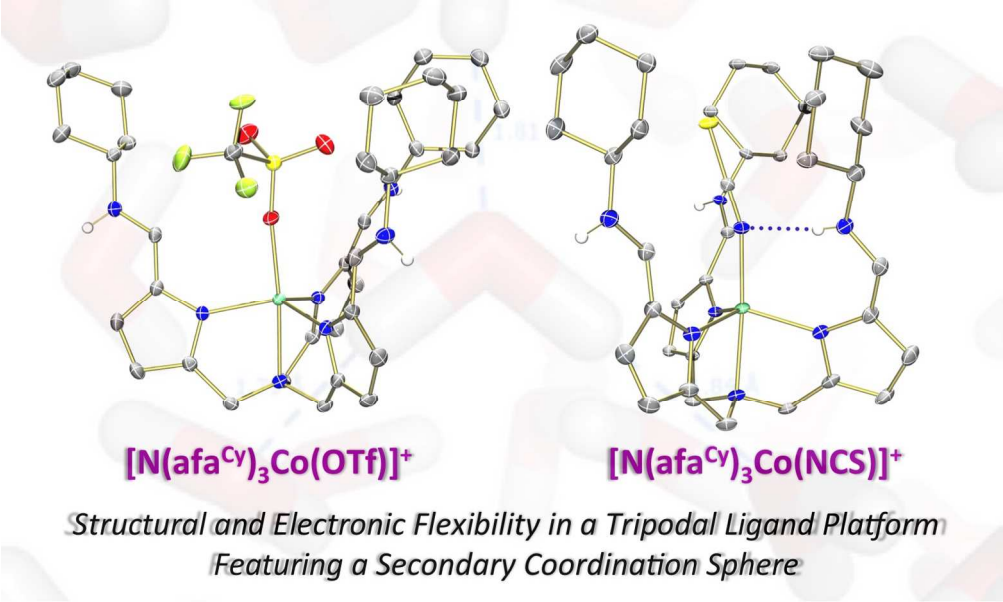

595x357mm (72 x 72 DPI)